View metadata, citation and similar papers at core.ac.uk
brought to you by CORE
provided by Repositorio Institucional de la Universidad de Oviedo

Angular stability of metasurface perfect absorbers: advances on the design and limitations on measurement

Humberto Fernández Álvarez[(1)], María Elena de Cos Gómez[(1)], and Fernando Las-Heras[(1)]
hfernandez@tsc.uniovi.es, medecos@tsc.uniovi.es, flasheras@tsc.uniovi.es
[(1)] Dpto. de Ingeniería Eléctrica Universidad de Oviedo. Edificio Polivalente, Mod. 8. E-33203 Gijón, Asturias, España.

***Abstract*- The aim of this contribution is twofold. On the one hand, some guidelines will be given in order to improve the metasurface absorbers' (MTAs) angular stability. In order to show that, two angularly stable MTAs are presented taking into consideration the common design specifications (resonance frequency, peak absorption, available dielectric materials and suitable bandwidth) that a designer has to meet. These MTAs are not only angularly stable but also its profile is extremely thin and hence, they can be conformed to whatever objects due to its flexibility. On the other hand, it will be provided a deep insight on the measurement limitations. A quasi-monostatic measurement set-up will be presented to perform measurements under both transverse electric (TE) and transverse magnetic (TM) polarizations varying the angle of incidence. The restrictions in the angular margin that can be measured according to the size of the manufactured finite MTA will be presented.**

I. INTRODUCTION

Metasurface perfect absorbers (MTAs) comprise unit-cells arranged in an infinite array [1]-[5]. Each unit-cell consists of a planar dielectric slab metallized on their top and bottom sides. Either one or both of the aforementioned metallized sides can be designed with a specific geometry. In this document, one side will be fully metallized and the other one will be designed with specific metallization geometry. MTAs are resonant structures, commonly used to absorb incident electromagnetic waves at their resonance frequency (f_r). For doing so, they are designed to match their equivalent surface impedance to the one of free space, so that the incident wave is fully transmitted. Moreover, the electromagnetic energy dissipation is mainly attained, at microwave frequencies using a lossy dielectric slab and at terahertz frequencies due to the metallization ohmic losses [6].

The behavior of the MTA depends on the dielectric material (its electrical properties (permittivity and permeability) and thickness), its metallization's geometry and its unit-cell's size (periodicity) [7]. These parameters completely determine the absorption peak, resonance frequency, bandwidth and angular stability of the MTA.

Their compact size, design flexibility and ease of manufacture gives rise to a great number of applications, such as RCS reduction [8], invisibility cloaks [9], sub-diffracting imaging [10], bolometers [11] and anti-collision radars [12] among others.

The narrow bandwidth and the angular instability of these MTAs are the main limitations that most authors try to overcome. The bandwidth is usually widened using multi-resonant structures that can be obtained, by scaling the unit-cells (either in the same layer [13] or in multiple-layers [8]) and/or including lumped resistors on the MTA's metallization [14]. The angular stability can be improved by introducing vias [15], increasing the dielectric permittivity [16] and/or compensating the angular dependency of the grounded dielectric slab by either, reducing its thickness or designing a more inductive grid impedance (impedance of the MTA's metallization geometry considering the underneath dielectric slab) [17]. However, the latter techniques usually give rise to a narrowing in the MTA's bandwidth. Therefore, a trade-off between MTA's angular stability and bandwidth must be stablished.

This work aims to improve the angular stability of MTA's from a designer point of view, who has to meet specific design requirements for the intended application, such as resonance frequency, MTA's profile (in which the dielectric thickness plays an important role and it is constrained to the available dielectric materials), absorption peak and suitable bandwidth. MTAs are ideally infinite structures but in practice, this size must be reduced and hence, arrays comprising several unit-cells are commonly considered. Therefore, a detailed discussion about the proper MTA's size and its implications for the measurements' accuracy retrieval will be presented.

II. PROPOSED MTAS

A. *MTA's geometry and characterization.*

In order to carry out a proper analysis of the MTA's angular stability, a full-wave FEM based commercial electromagnetic software is used, and the MTA's behavior under different polarizations (ϕ) and incidence angles (θ) of the incident wave is simulated Fig. 1(a). Consequently, the polarization angle is varied from 0º to 60º in steps of 20º for normal incidence and then, the incidence angle is also varied from 0º to 60º in steps of 20º. Moreover, this analysis is performed not only for the transverse electric (TE) polarization (electric field normal to the incidence plane) but also for transverse magnetic (TM) polarization (magnetic field normal to the incidence plane). In addition, the

frequency deviation (Δ_f) (the maximum shift of the resonance frequency for different polarization or incidence angles) and the stable bandwidth (B_s) (the bandwidth which ensures at least 50% absorption for all the polarization or incidence angles under analysis), are defined.

The unit-cells of the proposed MTAs are presented in Fig. 1(b) and Fig. 1(c). Both MTAs are designed to resonate in the C-band. The geometric parameters of the Pillar unit-cell (Fig. 1(b)) are: $p_1 = 14.37mm, p_2 = 13.74mm, h_e = 2mm, h_i = 1mm, w = 0.32mm$ and $l = 6.19mm$. On the other hand, the Star unit-cell geometric parameters (Fig. 1(c)) are: $p = 16.38mm, l_e = 3.86mm, l_i = 3.12mm, h_e = 1.9mm, h_i = 1.54mm, c = 0.82mm, g_e = 1.65mm$ and $g_i = 1.21mm$. A six-fold geometry is used for both MTAs since it has been previously demonstrated that hexagonal metasurfaces exhibit greater angular stability than the square based ones [18] and this is even more true for unit-cells with inductive metallization behavior.

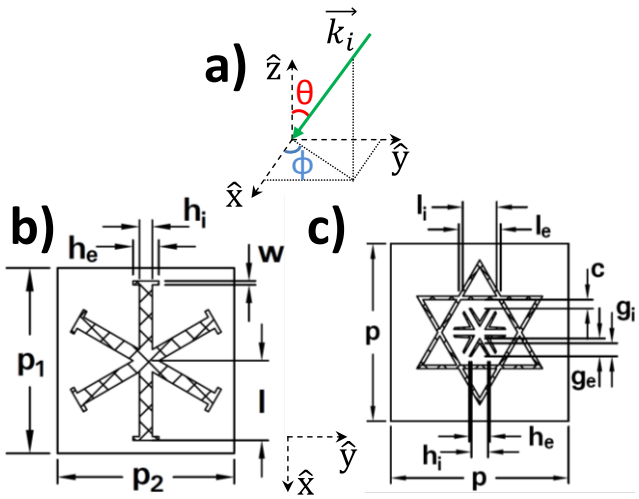

Fig. 1. Coordinate system highlighting the incident wave ($\vec{k_i}$), the polarization angle (ϕ) and the incidence angle (θ) (a). Pillar unit-cell geometry (b). Star unit-cell geometry (c).

The same dielectric material (ARLON 25N) and thickness (h=0.457mm) are considered for both MTAs in order to carry out a fair comparison between them. The resonance frequency, absorption peak and bandwidth, measured as full width at half maximum (FWHM), are shown in Table I. The Star MTA reaches a higher absorption peak than the Pillar one since its surface impedance is better matched to the free space impedance than the Pillar one. Thus, a minor amount of the incident wave energy is reflected at its interface being most of it transmitted and absorbed inside the lossy dielectric. Moreover, the Pillar MTA has a broader FWHM and higher resonance frequency than the Star one.

TABLE I
MTA's RESONANCE FREQUENCY, ABSORPTION PEAK AND FWHM

	f_r [GHz]	Absorption Peak [%]	FWHM [%]
Pillar (TE)	6.32	88.35	2
Star (TE)	6.08	98.37	1.53
Pillar (TM)	6.25	88.25	2
Star (TM)	6.01	98.23	1.53

B. MTA's angular stability.

The results of the MTA's angular stability analysis as regards Δ_f and B_s varying ϕ and θ are presented in Table II and Table III, respectively. The worst angular stability cases of both MTAs varying ϕ or θ are highlighted in Table II and Table III respectively and graphically depicted in Fig. 20. These cases represent the MTA's highest frequency deviation and narrowest stable bandwidth and hence, the MTA's operating specifications. From these operating specifications, it can be said that the Star MTA has a smaller frequency deviation and a broader stable bandwidth than the Pillar's one when the polarization angle of the incident wave varies (Table II). The frequency shift in both MTAs for polarization angle variations is mainly due to differences in metallization and unit-cells symmetry (six-fold vs four-fold). Indeed, this shift is more noticeable for the Pillar MTA since it has a rectangular, instead of square, periodicity. On the other hand, the Star MTA exhibits a better performance on both parameters (smaller Δ_f and wider B_s) than the Pillar MTA when the incidence angle changes (Table III). Since both MTAs use the same dielectric, which gives rise to the improvement in the angular stability is the metallization geometry of the Star MTA, as it is more inductive than the Pillar one.

TABLE II
ANGULAR STABILITY VARYING POLARIZATION ANGLE

	Δ_f [MHz]	Δ_f [%]	B_s [MHz]	B_s [%]
Pillar (TE)	126	2	59	0.93
Star (TE)	25	0.41	65	1.07
Pillar (TM)	130	2.06	87	1.39
Star (TM)	14	0.23	75	1.24

TABLE III
ANGULAR STABILITY VARYING INCIDENCE ANGLE

	Δ_f [MHz]	Δ_f [%]	B_s [MHz]	B_s [%]
Pillar (TE)	47	0.74	37	0.58
Star (TE)	32	0.53	44	0.73
Pillar (TM)	61	0.98	25	0.40
Star (TM)	54	0.90	32	0.53

The proposed MTAs offer more compact and thinner designs (total thickness $\sim\lambda/97$), with higher absorption performance when compared with other designs in the literature that use thicker dielectrics with larger losses.

Other considerations can be made in the previous MTAs in order to further improving their angular stability, such as:

- Introducing lumped components in the metallization's geometry to compensate the dependence of the grounded dielectric's impedance with the incidence angle.
- Adding substrates and/or superstrates to compensate the angular dependence of the MTA's equivalent surface impedance.

- Designing six-fold MTAs with a hexagonal periodicity.

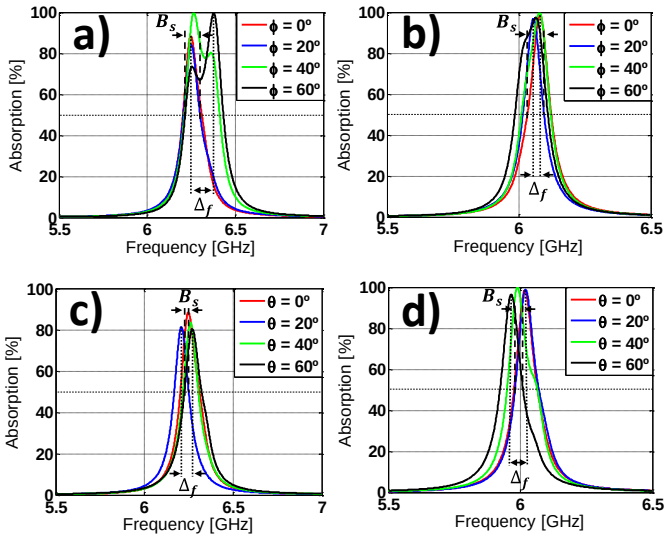

Fig. 2. The worst angular stability cases of the proposed MTAs varying polarization angle (Pillar (TM) (a) and Star (TE) (b)) or varying incidence angle (Pillar (TM) (c) and Star (TM) (d)).

III. Manufacturing and Measurement Considerations to Characterize MTAs in an Anechoic Chamber.

In practice, only finite sized MTAs can be manufactured. A first approximation in the number of unit-cells required to get a similar behavior to the ideal infinite case was proposed in [19], stablishing 100 unit-cells for a 2D metamaterial. However, the practical physical restrictions in the majority of applications do not allow fitting such amount of unit-cells. Moreover, in order to carry out a fair comparison between the simulation and measurement results, the latter must be retrieved under far-field conditions, taking into account that the larger the finite MTA, the further will be the distance to meet this condition. The physical restriction also determine the angular margin that can be properly measured using a finite MTA, since the scattered-field pattern of a square or rectangular prototype follows a "sinc" function and its main lobe narrows as the MTA size increases. This implies that the nulls of the MTA's scattered-field pattern appear at shorter incidence angles and hence, they impede the retrieval of proper measurements due to the reduction of the dynamic range. Consequently, the MTA size will be large enough to behave similar to its infinite counterpart, but at the same time small enough to meet the far-field conditions in the considered measurement set-up. In addition, the MTA's scattered-field pattern will determine the angular margin that will be able to be measured [20], [21].

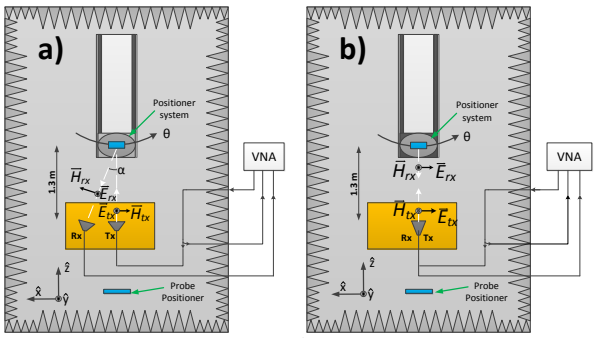

Fig 3. Measurement set-up for TE (a) and TM (b) polarization incidence wave.

The measurements will be carried out in an anechoic chamber, using a quasi-monostatic configuration of the transmission and reception antennas as it is shown in Fig 3. Narda 642 horn antennas, which have an aperture size of $115x110\ mm^2$, are chosen. The antennas are arranged to minimize the coupling between them.

For the sake of brevity and since this contribution aims to illustrate the challenges on measuring finite MTAs in a quasi-monostatic configuration in an anechoic chamber, only the Pillar MTA results will be shown. A finite MTA with 8x8 unit-cells was manufactured and the antennas were placed at 1.3m from the MTA so that the far-field condition for both MTA and antennas (antenna's aperture size $119x90\ mm^2$) is met. The set-up is calibrated measuring the scattered-field pattern of a metallic plate (acting as a perfect electric conductor (PEC)) with the same size as the finite MTA under test. These patterns are computed at the MTA's resonance frequency, giving a clue about the angular margin that will be able to be measured according to the available dynamic range in the retrieved measurements.

The MTA's scattered-field pattern and measurements for both TE and TM polarizations under different incidence angles are shown in Fig 4. From them, it can be appreciated the difference in the scattered-field pattern values between the PEC and the MTA, which indicates the absorption caused by the MTA. For the TE polarization, incidence angles from 0º to 10º can be measured, as the scattered-field pattern main lobe provides enough dynamic range. Then, a null in the pattern appears so it is not possible to distinguish between noise and the actual absorption. Around 18º, a side lobe of the scattered-field pattern increases the dynamic range, so several angles can be properly measured (18º, 20º and 22º). The same procedure is followed for getting the measurement results for TM polarization.

In order to increase the angular margin for which the MTA can be characterized using a quasi-monostatic configuration several techniques can be employed, such as using lens to couple as much incident energy as possible in the MTA, using only one antenna to transmit and receive the incident and reflected wave so as to avoid the unecessary coupling betweem them and/or manufacturing several MTA's with different sizes in order to shift their scattered-field pattern's side lobes and widen or narrow their main lobe. Moreover, taking several samples of the same measurements and performing an average, a background noise reduction can be obtained.

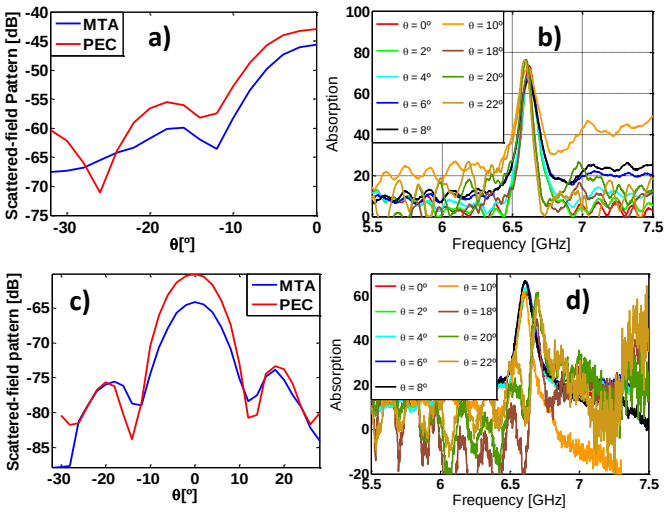

Fig 4. Scattered-field pattern at the MTA's resonance frequency (a,c) and MTA's measurements (b,d) for TE and TM configuration set-up, respectively.

Another interesting characterization will be the bistatic measurement which gives rise to a better understanding of how much the MTA really absorbs. However, actual radars do not works in such manner and bistatic measurements in anechoic chamber are difficult to arrange.

IV. Conclusions

Two main topics in the characterization of MTAs have been tackled in this contribution. On the one hand, the challenges on the design of angularly stable MTA have been described and some guidelines to improve the MTA's angular stability were given. Moreover, two angularly stable prototypes were presented using some of these guidelines, and additional ideas have been put forward for further studies. The angular stability of the proposed MTAs was analyzed for both polarization and incidence angle variations, giving justified reasons for their differentiated performance. On the other hand, the challenges on the practical characterization of these MTAs, using a quasi-monostatic configuration in anechoic chamber, have been presented, along with a relation between the MTA dimensions and the measurement limitations. Furthermore, measurements of a proposed MTA have been carried out in an anechoic chamber and a proper justification of the results was provided.

Acknowledgements

This work was supported by the Gobierno del Principado de Asturias/FEDER under Project GRUPIN14-114 and by the Ministerio de Economía y Competitividad under Project TEC2014-54005-P (MIRIIEM).

Referencias

[1] C.L. Holloway, et al. "An overview of the theory and applications of metasurfaces: The two-dimensional equivalents of metamaterials" *IEEE Antennas and Propagation Magazine*, vol. 54, no 2, pp. 10-35, 2012.

[2] Landy, N. I, et al. "Perfect metamaterial absorber," *Physical review letters*, vol. 100, no. 20, pp. 207402, 2008.

[3] H.F. Álvarez, et al. "A six-fold symmetric metamaterial absorber," *Materials*, vol. 8, no 4, p. 1590-1603, 2015,.

[4] H.F. Álvarez, "A Thin C-Band Polarization and Incidence Angle-Insensitive Metamaterial Perfect Absorber," *Materials*, 8, pp. 1666-1681, 2015.

[5] O. Ayop, et al. "Dual-band metamaterial perfect absorber with nearly polarization-independent," *Applied Physics A*, vol. 123, no. 1, pp. 63, 2017.

[6] X. Shen, et al. "Polarization-independent wide-angle triple-band metamaterial absorber," *Optics express*, vol. 19, no 10, p. 9401-9407, 2011.

[7] N. Zhang, et al. "A Planar Broadband Metamaterial Absorber with the Polarization Insensitive and Omnidirectional Absorption in the Min-infrared Regime," *PIERS Proceedings*, 2014.

[8] H. Yang, et al. "Low RCS metamaterial absorber and extending bandwidth based on electromagnetic resonances," *Progress In Electromagnetics Research M*, vol. 33, p. 31-44, 2013.

[9] D. Schurig, et al. "Metamaterial electromagnetic cloak at microwave frequencies," *Science*, vol. 314, no 5801, p. 977-980, 2006.

[10] N. Fang, et al. "Sub-diffraction-limited optical imaging with a silver superlens," *Science*, vol. 308, no 5721, p. 534-537, 2005.

[11] K. Du, et al. "Wavelength and thermal distribution selectable microbolometers based on metamaterial absorbers," *IEEE Photonics Journal*, vol. 7, no 3, p. 1-8, 2015.

[12] Y. Urzhumov, et al. "Electronically reconfigurable metal-on-silicon metamaterial," *Physical Review B*, vol. 86, no 7, p. 075112, 2012.

[13] L. Hao, et al. "Extending the bandwidth of electric ring resonator metamaterial absorber," *Chinese Physics Letters*, vol. 28, no 3, p. 034204, 2011.

[14] S. Li, et al. "Wideband, thin, and polarization-insensitive perfect absorber based the double octagonal rings metamaterials and lumped resistances," *Journal of Applied Physics*, vol. 116, no 4, p. 043710, 2014.

[15] S.A. Tretyakov, "Thin absorbing structure for all incidence angles based on the use of a high-impedance surface," *Microwave and Optical Technology Letters*, 2003, vol. 38, no 3, p. 175-178.

[16] O. Luukkonen, et al. "A thin electromagnetic absorber for wide incidence angles and both polarizations," *IEEE transactions on antennas and propagation*, vol. 57, no 10, p. 3119-3125, 2009.

[17] L. Akhoondzadeh-Asl, et al. "Influence of element shape on the bandwidth of artificial magnetic conductors," *Journal of Electromagnetic Waves and Applications*, vol. 21, no 7, p. 929-946, 2007.

[18] M.E. de Cos and F. Las-Heras, "On the advantages of loop-based unit-cell's metallization regarding the angular stability of artificial magnetic conductors," *Applied Physics A*, vol. 118, no 2, p. 699-708, 2015.

[19] M. Lapine and S. Tretyakov, "Contemporary notes on metamaterials," *IET microwaves, antennas & propagation*, vol. 1, no 1, pp. 3-11, 2007.

[20] H. F. Alvarez, et al. "Angular Stability of Metasurfaces: Challenges Regarding Reflectivity Measurements [Measurements Corner]," *IEEE Antennas and Propagation Magazine*, vol. 58, no 5, pp. 74-81, 2016.

[21] Y. Alvarez et al. "RCS measurement setup for periodic-structure prototype characterization," *IEEE Antennas and Propagation Magazine*, vol. 52, no 3, p. 100-106, 2010.